UC Office of the President
Recent Work

Title
Relaxed c-plane InGaN layers for the growth of strain-reduced InGaN quantum wells

Permalink
https://escholarship.org/uc/item/5kv6j5dt

Journal
Semiconductor Science and Technology, 30(10)

Authors
Hestroffer, K.
Wu, F.
Li, H.
et al.

Publication Date
2015

Peer reviewed

eScholarship.org Powered by the California Digital Library
University of California

IOPscience iopscience.iop.org

Relaxed *c*-plane InGaN layers for the growth of strain-reduced InGaN quantum wells

This content has been downloaded from IOPscience. Please scroll down to see the full text.

View the table of contents for this issue, or go to the journal homepage for more

Download details:

IP Address: 169.236.9.179
This content was downloaded on 25/11/2015 at 20:55

Please note that terms and conditions apply.

2015 Semicond. Sci. Technol. 30 105015

IOP Publishing | Semiconductor Science and Technology

Semicond. Sci. Technol. **30** (2015) 105015 (6pp) | doi:10.1088/0268-1242/30/10/105015

Relaxed *c*-plane InGaN layers for the growth of strain-reduced InGaN quantum wells

Karine Hestroffer[1], Feng Wu[2], Haoran Li[1], Cory Lund[1], Stacia Keller[1], James S Speck[2] and Umesh K Mishra[1]

[1] Electrical and Computer Engineering Department, University of California, Santa Barbara, CA 93106, USA
[2] Materials Department, University of California, Santa Barbara, CA 93106, USA

E-mail: hestroffer@ece.ucsb.edu

Received 20 February 2015, revised 23 June 2015
Accepted for publication 21 July 2015
Published 1 September 2015

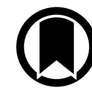

Abstract

A fully relaxed $In_{0.1}Ga_{0.9}N$ layer was grown by plasma-assisted molecular beam epitaxy on *c*-plane GaN using a grading technique. The growth of the graded InGaN layer in the intermediate regime enabled a smooth surface without the accumulation of In droplets. Transmission electron microscopy images show that the relaxation occurs through the formation of a high density of threading dislocations (TDs). Despite the presence of these TDs, relaxed InGaN films were then successfully used as a pseudo-substrate for the growth of InGaN/GaN quantum wells which luminesced at room temperature.

Keywords: InGaN, molecular beam epitaxy, strain relaxation, quantum wells

(Some figures may appear in colour only in the online journal)

1. Introduction

(In,Al,Ga)N semiconductor alloys have revolutionized both the optoelectronic [1, 2] and the electronic [3] industries. One of the remaining challenges lies in the realization of InGaN structures with high (i.e. $\geqslant$ 25%–30%) In content, which is hampered by two important issues. First, GaN and InN present a lattice mismatch as high as 10%. Lattice mismatch induces misfit strain which relaxes through the formation of defects above a critical thickness. The larger the In content in the InGaN film, the smaller the critical thickness [4, 5]. Misfit strain also hinders In incorporation through the compositional pulling effect [6–9]. GaN and InN additionally present a significant difference in thermal stability. While GaN dissociation becomes significant only around 750 °C [10], InN begins decomposing around 500 °C [11]. As a consequence, the typical InGaN growth temperature in plasma-assisted molecular beam epitaxy (PAMBE) is about about 100 °C lower than the ideal GaN growth temperature [12]. A higher In content requires lower growth temperatures which can be detrimental to the overall crystal quality.

These issues have nurtured the idea of using a relaxed $In_xGa_{1-x}N$ layer as a pseudo-substrate for the growth of $In_zGa_{1-z}N$-based structures where $z \geqslant x$ [8]. By doing so, the lattice mismatch between $In_zGa_{1-z}N$ and the substrate is reduced, as compared to the mismatch between $In_zGa_{1-z}N$ and a GaN substrate or between $In_zGa_{1-z}N$ and compressively strained $In_xGa_{1-x}N$. A lower mismatch would allow for enhancing the In incorporation, for increasing the critical thickness of the $In_zGa_{1-z}N$ film and also for lowering the piezoelectric component of the polarization. More generally, by controlling the lattice of the substrate, one gains control over the piezoelectric field inside the top structure.

Achieving full or even partial relaxation of an InGaN layer via an abrupt transition has proven to be challenging because it is generally accompanied by the formation of a high density of V-defects and pits that degrade the structural and optical quality of the layer [13]. Alternative solutions involving complex multi-step procedures have been proposed and demonstrated [14–17]. Recently, a fully relaxed $In_{0.1}Ga_{0.9}N$ layer was achieved on GaN through PAMBE growth of a metamorphic InGaN buffer with a slow grade of about 2% per 100 nm containing GaN interlayers every 100 nm [16]. The insertion of GaN interlayers most likely allowed for protection of the InGaN layers while raising the temperature of the substrate from about 570 °C (InGaN

 © 2015 IOP Publishing Ltd Printed in the UK

growth temperature) to 700 °C, a temperature required to desorb the metallic In accumulated on the surface during the growth of the previous 100 nm of InGaN. This strategy is however time-consuming, since each GaN interlayer cycle (GaN growth, temperature raise, temperature decrease back) takes about 25 min. To reach a 20% In mole fraction InGaN buffer, 10 of these cycles are required, which are typically worth over 4 h of growth time. In addition, around 570 °C, Ga adatom mobility is low, resulting in GaN interlayers of poor crystalline quality which may deteriorate the layer.

In the present work, a fully relaxed $In_{0.1}Ga_{0.9}N$ layer is achieved by PAMBE through the growth of a graded metamorphic buffer without GaN interlayers, allowing for a time-saving, straight-forward continuous epitaxial procedure. This structure is made possible by growing the InGaN buffer near the stoichiometric region of the growth diagram, which allows for a smooth surface without accumulation of In droplets. The relaxed InGaN layer is then used as a pseudo-substrate for the growth of $In_{0.1}Ga_{0.9}N$ quantum wells (QWs) embedded in GaN barriers which exhibit luminescence at room temperature.

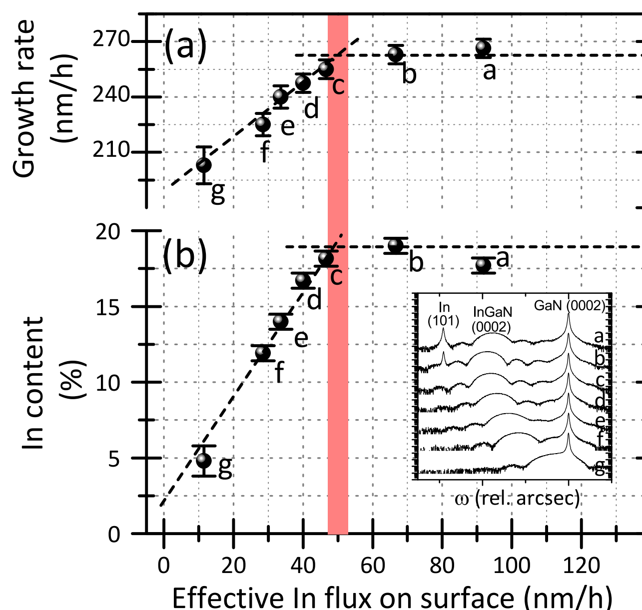

Figure 1. (a) Growth rate and (b) In content of InGaN layers as a function of the effective In flux, respectively determined from the fringe spacing and the 0002 InGaN peak position of the ω-2θ XRD scans shown in the inset.

2. Experimental procedure

Samples were grown in a Varian Gen II MBE system equipped with two Ga and one In solid-source effusion cells, and a rf-plasma nitrogen source. The rf-plasma nitrogen source was operated at 250 W with a constant N_2 flux of 0.7 sccm. This flow rate and rf power corresponded to a growth rate of about 285 nm h^{-1}. The pressure during growth was 2.4×10^{-5} Torr. During growth, the surface of the samples was characterized using reflection high energy electron diffraction (RHEED). Samples were then analyzed by high-resolution x-ray diffraction ω-2θ scans, and (ω-2θ)-ω reciprocal space maps (rsm) were recorded on a triple-axis philips/panalytical materials research diffractometer. Atomic force microscopy (AFM) images were recorded in tapping mode using an Asylum MFP3D instrument. Photoluminescence (PL) spectra were acquired using the 325 nm line of a He–Cd laser at room temperature. Transmission electron microscopy (TEM) was performed on a FEI G2 Tecnai microscope operated at 200 kV.

3. Results and discussion

3.1. Flux calibration

Because of the stronger Ga–N bond as compared to the In-N one, when growing InGaN by PAMBE, Ga adatoms incorporate on the metal sites preferentially while In atoms fill the remaining ones. The In mole fraction of the grown InGaN layer is therefore controlled by adjusting the Ga flux while In species are the one used to create the metal excess. Yet, around 570 °C the In desorption rate is lower than the In-N bond decomposition rate, making it difficult to avoid In accumulation on the surface [18]. The first part of this work aims at identifying the region of the growth diagram corresponding to the effective stoichiometry between the active nitrogen and the metal species in order to avoid In accumulation on the surface. To do so, a series of InGaN layers was grown for 8 min at 575 °C as measured with an optical pyrometer calibrated versus the melting point of Al. The substrates used were Ga-face GaN templates prepared by MOCVD on sapphire, which typically exhibit a dislocation density of about 10^8 cm^{-2}. For each sample, the Ga flux was kept constant at 215 nm h^{-1} and the In beam equivalent pressure was changed such that the effective In flux on the surface at 575 °C ranged from 10 to 90 nm h^{-1}. The effective In flux on the surface represents the incident In flux less the In flux desorbed from the surface plus the In flux released through partial decomposition of the InGaN layer. It was estimated by comparison of samples grown at 575 °C with samples grown at 400 °C, a temperature at which both In-N decomposition and In desorption can be neglected (not shown here). Figure 1 presents the growth rate (a) and the In content (b) of each of these samples as a function of the effective In flux on the surface. Growth rates and In contents were respectively determined from the fringe spacing and the 0002 InGaN peak position of the ω-2θ XRD scans shown in the inset. As verified from rsm obtained from the asymmetric $11\bar{2}4$ reflection (not shown here), all InGaN films grown under the above-described conditions are fully strained to the GaN substrate.

For the higher In fluxes (samples a and b), both the growth rate and the In content are constant. On the 0002 ω-2θ XRD scans shown in inset, besides the GaN, the InGaN and the fringe peaks, a peak due to metallic In is also visible. This peak indicates the presence of In droplets on the surface, a characteristic of In-rich growth conditions. In the lower In

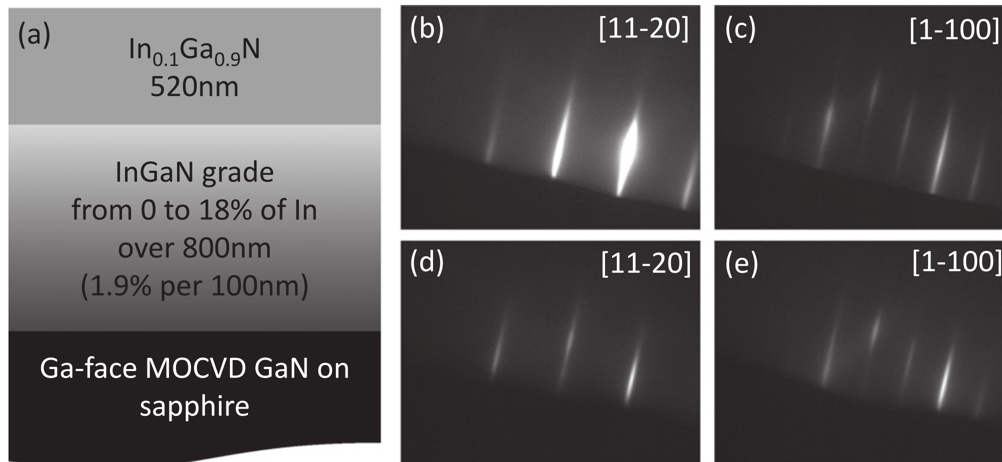

Figure 2. (a) Scheme of the structure grown to achieve a relaxed $In_{0.1}Ga_{0.9}N$ layer; (b) and (c) RHEED patterns respectively observed along $[11\bar{2}0]$ and $[1\bar{1}00]$ azimuths at the end of the InGaN grade; (d) and (e) RHEED patterns respectively observed along $[11\bar{2}0]$ and $[1\bar{1}00]$ azimuths at the end of the $In_{0.1}Ga_{0.9}N$ top layer growth.

flux range (samples d–g), the growth rate and the In content decrease linearly with the In flux. ω-2θ XRD scans of these samples do not exhibit a metal In peak. These growth conditions correspond to a N-rich regime. The transition region between the metal-rich and the N-rich zones, marked by the red rectangle, corresponds to stoichiometry between the metal and the active N species. In the present case, when using a Ga flux of 215 nm h^{-1}, stoichiometric conditions are attained with an effective In flux on the surface of 50 nm h^{-1}, leading to a growth rate of about 265 nm h^{-1}. This growth rate is lower than the growth rate of 285 nm h^{-1} expected from the *N* plasma source settings because of the non-negligible In-N decomposition rate at 575 °C.

3.2. Relaxed $In_{0.1}Ga_{0.9}N$ layer

The second part of this work focuses on the achievement of a relaxed InGaN layer. Figure 2 (a) presents a schematic of the grown structure which is composed of two parts: (i) a graded InGaN buffer and (ii) a thick InGaN layer with constant composition. The whole structure was grown at 575 °C on a template of Ga-face MOCVD GaN/Al_2O_3 which presents a miscut of 0.2°. In order to grade the In content in the InGaN buffer, the Ga flux was lowered from 280 to 205 nm h^{-1}. To remain close to stoichiometric conditions the effective In flux on the surface was correspondingly increased. The InGaN was graded with an increase of 1.8% of In every 100 nm. Figures 2 (b) and (c) present the RHEED pattern observed at the end of the InGaN grade. The pattern is streaky and bright. It exhibits a 1× structure along the $[11\bar{2}0]$ azimuth and a 3× structure along the $[1\bar{1}00]$ azimuth which constitutes the signature of metal-face InGaN ($\sqrt{3} \times \sqrt{3}$) surface reconstruction [19]. On top of the 800 nm thick graded buffer, $In_{0.1}Ga_{0.9}N$ was grown for 2 h using a Ga flux of about 240 nm h^{-1} and an effective In flux on the surface of about 35 nm h^{-1}. At the end of this thick $In_{0.1}Ga_{0.9}N$ film growth, the RHEED pattern still exhibited the InGaN ($\sqrt{3} \times \sqrt{3}$) surface reconstruction (figures 2 (d) and (e)). Let us note that values of Ga and In fluxes are should be taken with caution since the exact evolution of the Ga and In beam equivalent pressures were not monitored during the growth of the grade.

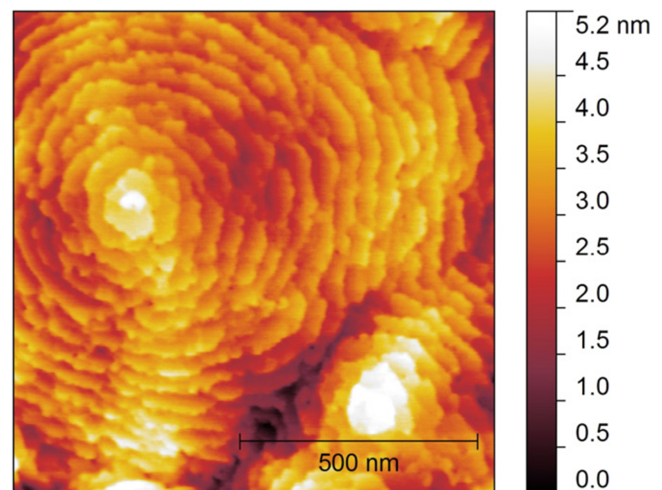

Figure 3. 1×1 μm^2 AFM image of the surface, exhibiting spiral growth. The rms surface roughness is 0.75 nm.

Figure 3 presents the 1×1 μm^2 AFM image of the sample's surface acquired after growth. The surface exhibits spiral steps and a root mean square (rms) surface roughness as low as 0.75 nm on this area. On larger areas, namely 5×5 and 10×10 μm^2, the rms surface roughness is about 4 nm. The formation of spirals is characteristic of a step-flow growth mode mediated by the presence of dislocations [20, 21]. In droplets were not observed, indicating that the effective total metal fluxes remained close to the effective active *N* flux throughout the growth of the entire 1.3 μm thick structure. For the growth of GaN by PAMBE, three regimes are usually observed: a N-rich regime that leads to rough surfaces, a droplet regime (very metal-rich) that leads to smooth surfaces but accumulates Ga droplets, and an intermediate Ga-stable regime [22]. The intermediate regime is a slightly metal-rich growth regime under which up to ~2.5 monolayers [23] of Ga adatoms cover the surface acting as a surfactant [24, 25].

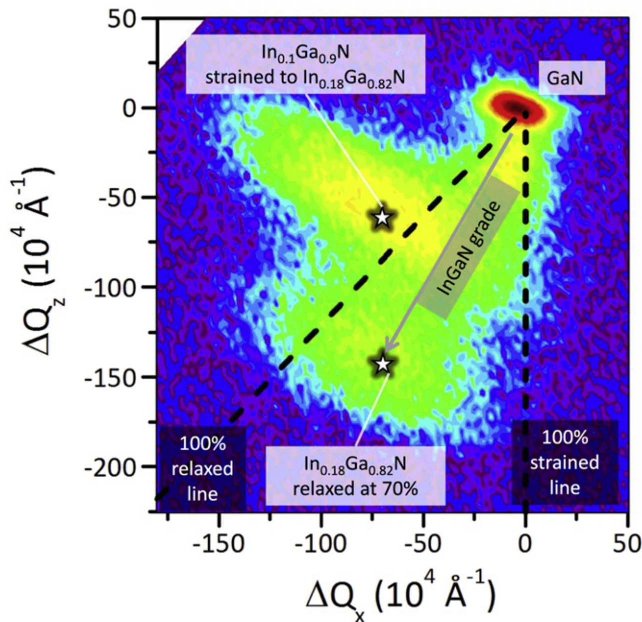

Figure 4. Reciprocal space map obtained around GaN $11\bar{2}4$ reflection. The graded buffer (see figure 2 (a)) reaches a maximal In mole fraction of 0.18 and a maximum relaxation of 70%. The 520-nm thick top InGaN layer (see figure 2 (a)) has an In mole fraction of about 0.1 and is under slight tensile strain imposed by the underneath graded buffer, near full relaxation (oblique black dashed line).

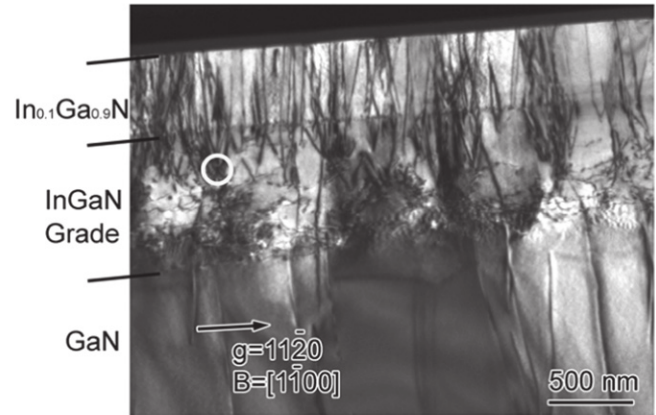

Figure 5. TEM image illustrating the high density of threading dislocations that spread through the graded InGaN buffer and the top thick $In_{0.1}Ga_{0.9}N$ layer.

Similarly, for InGaN growth, the surfactant behavior of In adatoms has already been reported [19, 26, 27]. Most likely in our case, by changing the Ga and In fluxes in parallel, we deviated from strictly stoichiometric conditions but remained in the InGaN intermediate growth regime, preventing the accumulation of In droplets. A detailed diagram of InGaN growth regimes is currently under preparation and will be published elsewhere [28].

A rsm obtained around GaN $11\bar{2}4$ reflection is shown in figure 4. As determined by the positions of the different peaks in the reciprocal space, the graded buffer reaches a maximum In mole fraction of 0.18 and a maximum relaxation of 70%. The 520 nm thick top InGaN layer has an In mole fraction of about 0.10 and is under slight tensile strain imposed by the underneath graded buffer, near full relaxation. The composition of the thick top layer was confirmed by energy-dispersive x-ray spectroscopy which revealed an average In mole fraction of 0.096.

To investigate the origin of this relaxation, the sample was analyzed by TEM. Figure 5 shows a cross-sectional bright field micrograph of the $(11\bar{2}0)$ plane. The image highlights the generation of up to 10^{10} threading dislocations (TDs) per cm^2 of both pure edge and mixed types throughout the InGaN grade. This is about two orders of magnitude larger than the density of dislocations of the GaN substrate. Interestingly, as indicated by the white circle, the TDs seem not to be generated directly at the InGaN/GaN interface but only after the growth of an InGaN grade thickness of about 500 nm where the In mole fraction is about 0.12. In addition, a significant fraction of the TDs forming in the upper part of the grade appear to be inclined rather than perfectly aligned along the [0001] direction. Generally, in a given crystal, pre-existing TDs glide through the formation of misfit dislocation (MD). This glide is possible when shear stress is present on the TD glide plane and allows the bending of these TDs. For wurtzite nitride materials, it has been established that the most favorable slip plane is the (0001) plane [29, 30]. For this reason, when growing on the *c*-plane, bending of TDs does not typically occur through dislocation glide. The relaxation may rather be related to an effective climb of edge dislocations, a phenomenon observed and described in compressively strained AlGaN layers [29, 31]. Using the formula $\bar{\epsilon_{\rm pl}} = \frac{1}{4} b \rho_{\rm TD} h \tan \alpha$ given in [29], one can estimate the average plastic relaxation $\bar{\epsilon_{\rm pl}}$ for the grade. Considering a Burgers vector length $b = 0.318$ nm (GaN in-plane lattice parameter), a TD density $\rho_{\rm TD} = 1 \times 10^{10}\ {\rm cm}^{-2}$ (determined from plane-view TEM images, not shown here), a grade thickness $h = 750$ nm and a dislocation inclination angle $\alpha = 15°$, we get $\bar{\epsilon_{\rm pl}} \approx 0.0016$. Based on the rsm in figure 4, we observed that the grade reaches an In mole fraction of 0.18 and is relaxed at 70%. The misfit accommodated can therefore be evaluated as $\epsilon = 0.7 \cdot (a_{\rm In_{0.18}Ga_{0.82}N} - a_{\rm GaN})/(a_{\rm In_{0.18}Ga_{0.82}N}) = 0.014$. The misfit plastically relieved through the formation of TDs is only about one tenth of the misfit effectively relieved, which suggests the occurrence of additional mechanisms in the relaxation of the grade. These additional mechanisms may include dislocation glide on pyramidal planes as observed in [32]. Additional defects can also be observed at the InGaN/GaN interface, the nature of which is not yet fully understood. Dedicated work is currently in progress to investigate these questions.

Despite the presence of a high density of TDs, PL signal from the grown structure was detected at room temperature and peaks at 445 nm (2.8 eV). PL spectrum of this sample is not shown but that of another similar relaxed InGaN pseudo-substrate sample, used in the second part of this work, is (see figure 6). Based on Vegard's law, a 445 nm emission wavelength corresponds to an In content of about 15%. This is larger than the average In content of 10% determined from the rsm in figure 4. Both theoretically [33] and experimentally [9], the occurrence of phase separation has been shown to be

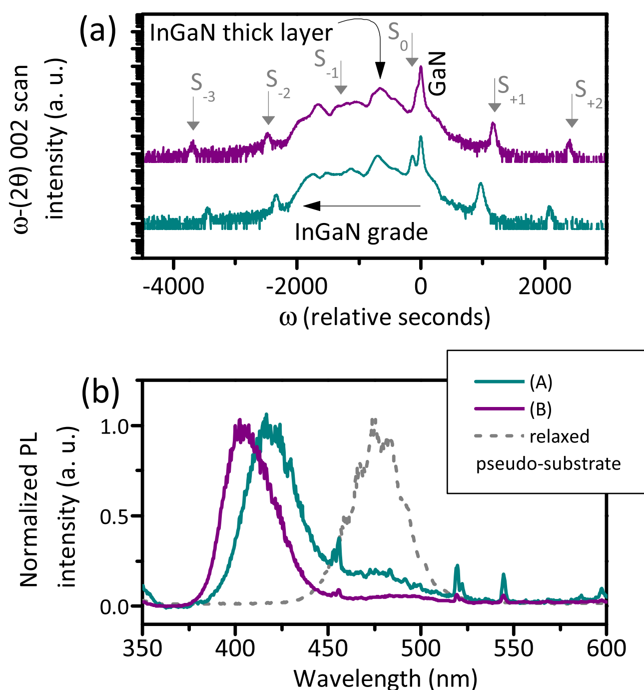

Figure 6. (a) GaN 0002 ω-2θ XRD scans from the two QW samples; (b) corresponding normalized room-temperature PL (colored lines) and PL signal from the relaxed InGaN pseudo-substrate (gray dashed line).

strongly related to strain relaxation in InGaN films. It is possible in our case that the luminescence arise from richer In zones forming through such phase separation. Preliminary cathodoluminescence analyses tend to confirm this hypothesis, showing a spatially non-homogeneous origin of the luminescence.

3.3. InGaN QWs grown on relaxed InGaN pseudo-substrate.

In the last part of this work, relaxed InGaN layers such as the one described in the previous section are used as a pseudo-substrate for the growth of InGaN QWs embedded in GaN barriers. To do so, the growth procedure described in section 3 was repeated on a two inch MOCVD GaN/sapphire wafer. Square centimeter pieces were then diced from the center of this wafer, cleaned and reloaded into the growth chamber. Two samples were grown with 20 InGaN QWs embedded in GaN barriers, each.

Figure 6 (a) presents ω-2θ XRD scans around GaN 0002 reflection for these two samples. The GaN substrate peak is centered at 0 s. The InGaN grade extends to the left of the GaN peak down to about −2000 s. The top thick InGaN layer raises at about −660 s. Satellites peaks related to the InGaN QW/GaN barrier superlattice can be clearly distinguished up to +2nd and −3rd orders which indicates good InGaN/GaN interfaces. As determined from dynamical simulations performed with these scans the QWs contain 10% In and have thicknesses of 2.4 nm (sample A) and 0.9 nm (sample B). The GaN barriers have thicknesses of 12.7 nm for both samples.

Figure 6 (b) shows the normalized room temperature PL signal detected from the pseudo-substrate itself (gray dashed line) and that from the two QW samples (colored lines). Both samples present one strong peak originating from the QWs and a shoulder with a weaker intensity arising from the pseudo-substrate. For sample A, the main peak raises at 418 nm while for sample B the QWs luminesce at 406 nm. This 12 nm red-shift observed for sample A is most likely related to the decrease of the confinement inside thicker QWs. Analyzing recombination mechanisms in InGaN QWs and their dependence on structural parameters such as the thickness of the well requires to both take into account internal electrostatic fields and consider the possible role of compositional fluctuations [34]. Such analyses go beyond the scope of this work, which stands as the first report on luminescing MBE-grown InGaN QWs on relaxed InGaN pseudo-substrates and lays the groundwork for the realization of novel InGaN-based structures and devices in which the control of the strain is crucial.

4. Conclusion

In conclusion, relaxed $In_{0.1}Ga_{0.9}N$ layers with a smooth surface were grown by PAMBE. More generally, a straightforward procedure for the growth of relaxed $In_xGa_{1-x}N$ layers has been established. Such relaxed InGaN layer has then been used as a pseudo-substrate for the growth of InGaN QWs embedded in GaN barriers. Despite the presence of a large density of TDs, the QWs emit at room temperature. To our knowledge, this work is the first report on luminescence of InGaN QWs grown by MBE on relaxed InGaN pseudo-substrates.

Acknowledgments

The authors gratefully acknowledge funding support from the Office of Naval Research (Dr Paul Maki, program manager), CAST, and the Solid State Lighting and Energy Electronics Center (SSLEEC) at UCSB. This work made use of Central Facilities at UCSB supported by the NSF MRSEC program under Award no. DMR-1121053. A portion of this work was done in the University of California Santa Barbara Nanofabrication Facility, part of the NSF-funded National Nanotechnology Infrastructure Network. Fruitful discussions with Elaheh Ahmadi, David Browne and Dr Erin Young are acknowledged.

References

[1] Nakamura S and Chichibu S F 2000 *Introduction to Nitride Semiconductor Blue Lasers and Light Emitting Diodes* (Boca Raton, FL: CRC Press)
[2] Jani O, Ferguson I, Honsberg C and Kurtz S 2007 *Appl. Phys. Lett.* **91** 132117
[3] Pearton S J and Ren F 2000 *Adv. Mater.* **12** 1571
[4] Matthews J W and Blakeslee A E 1974 *J. Cryst. Growth* **27** 118

[5] Holec D, Costa P M F J, Kappers M J and Humphreys C J 2007 *J. Cryst. Growth* **303** 314
[6] Kawaguchi Y, Shimizu M, Hiramatsu K and Sawaki N 1997 *Mater. Res. Soc. Symp. Proc.* 449 89
[7] Pristovsek M, Stellmach J, Leyer M and Kneissl M 2009 *Phys. Status Solidi* c **6** S565
[8] Sharma T K and Towe E 2010 *J. Appl. Phys.* **107** 024516
[9] Mueller M, Smith G D W, Gault B and Grovenor C R M 2012 *Acta Mater.* **60** 4277
[10] Grandjean N, Massies J, Semond F, Karpov S Y and Talalaev R A 1999 *Appl. Phys. Lett.* **74** 1854
[11] Saitoh H, Utsumi W, Kaneko H and Aoki K 2007 *J. Cryst. Growth* **300** 26
[12] Nath D N, Gr N, Ringel S A and Rajan S 2011 *J. Vac Sci. Technol.* B **29** 021206
[13] Wang H, Jiang D S, Jahn U, Zhu J J, Zhao D G, Liu Z S, Zhang S M, Qiu Y X and Yang H 2010 *Physica* B **405** 4668
[14] Chua C L, Yang Z, Strittmatter A and Teepe M R 2011 Relaxed ingan/algan templates *USA Patent* patent 2011/0150017 a1
[15] Liu Y *et al* 2012 *J. Vac Sci. Technol.* B **30** 030603
[16] Daeubler J, Aidam R, Koehler K, Kirste L, Passow T, Kunzer M and Wagner J 2013 GaInN on GaN buffer layer with enlarged in-place lattice parameter as template for strain-engineered long wavelength GaInN QW emitters *Int. Conf. On Nitride Semiconductor 2013* (*ICNS—10*) (*Washington DC, USA*) (Oral presentation)
[17] Islam S M, Protasenko V, Xing H G, Jena D and Verma J 2014 Use of graded $Ga_xIn_{1-x}N$ as a buffer layer for PAMBE growth of thick InN *Int. Conf. On Molecular Beam Epitaxy* (*ICMBE—18*) (*Flagstaff, USA*) (Oral presentation)
[18] Ive T, Brandt O, Ramsteiner M, Giehler M, Kostial H and Ploog K H 2004 *Appl. Phys. Lett.* **84** 1671
[19] Chen H, Feenstra R M, Northrup J E, Zywietz T, Neugebauer J and Greve D W 2000 *J. Vac Sci. Technol.* B **18** 2284
[20] Heying B, Tarsa E J, Elsass C R, Fini P, DenBaars S P and Speck J S 1999 *J. Appl. Phys.* **85** 6470
[21] Skierbiszewski C, Siekacz M, Perlin P, Feduniewicz-Zmuda A, Cywinski G, Grzegory I, Leszczynski M, Wasilewski Z R and Porowski S 2007 *J. Cryst. Growth* **305** 346
[22] Heying B, Averbeck R, Chen L F, Haus E, Riechert H and Speck J S 2000 *J. Appl. Phys.* **88** 1855
[23] Adelmann C, Brault J, Mula G and Daudin B 2003 *Phys. Rev.* B **67** 165419
[24] Neugebauer J, Zywietz T K, Scheffler M, Northrup J E, Chen H and Feenstra R M 2003 *Phys. Rev. Lett.* **90** 056101
[25] Adelmann C, Brault J, Jalabert D, Gentile P, Mariette H, Mula G and Daudin B 2002 *J. Appl. Phys.* **91** 9638
[26] Widmann F, Daudin B, Feuillet G, Pelekanos N and Rouvire J L 1998 *Appl. Phys. Lett.* **73** 2642
[27] Adelmann C, Langer R, Feuillet G and Daudin B 1999 *Appl. Phys. Lett.* **75** 3518
[28] Hestroffer K, Li H, Lund C, Keller S, Speck J S and Mishra U K 2015 Plasma assisted molecular beam epitaxy growth diagram of InGaN on (0001) GaN for the optimized synthesis of InGaN compositional grades *Phys. Status Solidi* a submitted
[29] Romanov A E and Speck J S 2003 *Appl. Phys. Lett.* **83** 2569
[30] Young E C, Wu F, Romanov A E, Tyagi A, Gallinat C S, DenBaars S P, Nakamura S and Speck J S 2010 *Appl. Phys. Express* **3** 011004
[31] Romanov A E, Young E C, Wu F, Tyagi A, Gallinat C S, Nakamura S, DenBaars S P and Speck J S 2011 *J. Appl. Phys.* **109** 103522
[32] Srinivasan S, Geng L, Liu R, Ponce F A, Narukawa Y and Tanaka S 2003 *Appl. Phys. Lett.* **83** 5187
[33] Liu J Z and Zunger A 2008 *Phys. Rev.* B **77** 205201
[34] Waltereit P, Brandt O, Ringling J and Ploog K 2001 *Phys. Rev.* B **64** 245305